

Acetylation of Glycerol over Highly Stable and Active Sulfated Alumina Catalyst: Reaction Mechanism, Kinetic Modeling and Estimation of Kinetic Parameters

ARUN PANKAJAKSHAN, SATYANARAYANA MURTY PUDI, PRAKASH BISWAS

Department of Chemical Engineering, Indian Institute of Technology Roorkee, Roorkee, 247 667, Uttarakhand, India

Received 2 March 2017; revised 10 October 2017; accepted 21 November 2017

DOI 10.1002/kin.21144

Published online in Wiley Online Library (wileyonlinelibrary.com).

ABSTRACT: The Langmuir–Hinshelwood–Hougen–Watson (LHHW) kinetic model was developed for acetylation of glycerol over highly stable and active 2 M $\text{SO}_4^{2-}/\gamma\text{-Al}_2\text{O}_3$ catalyst. The apparent reaction rate constants were determined by numerically solving the differential rate equations using ode23 tool in MATLAB coupled with the genetic algorithm optimization technique. The estimated rate constants were used to obtain the activation energy and pre-exponential factor by using the Arrhenius equation. The estimated activation energy for direct acetylation of glycerol to monoacetylglycerol and diacetylglycerol was 7.2 kJ mol^{-1} , for acetylation of monoacetylglycerol to diacetylglycerol was 37.1 kJ mol^{-1} , and for acetylation of diacetylglycerol to triacetylglycerol was 26.6 kJ mol^{-1} , respectively. © 2017 Wiley Periodicals, Inc. *Int J Chem Kinet* 1–14, 2017

INTRODUCTION

Biodiesel production can be economically more viable by the value addition of surplus amounts of glycerol obtained as by-product [1,2]. Among the various glycerol

value addition processes proposed such as hydrogenolysis, etherification, selective oxidation, fermentation, dehydration, carboxylation, esterification etc., esterification of glycerol with acetic acid is a promising route. The esterification of glycerol with acetic acid produces monoacetylglycerol (MAG), diacetylglycerol (DAG), and triacetylglycerol (TAG). These products have a significant commercial importance. MAG is widely used as a food additive; in combination with DAG and TAG,

Correspondence to: Prakash Biswas; e-mail: prakbfch@iitr.ac.in, prakashbiswas@gmail.com.

© 2017 Wiley Periodicals, Inc.

MAG finds applications in the manufacture of dyes, softening agents, and plasticizers. Moreover, DAG and TAG are excellent fuel additives, which on addition to fuel reduces the viscosity of fuel and increases engine efficiency and also these components improve the antiknocking properties of gasoline when blended [3].

In the past two decades, various catalysts have been developed and their performances were evaluated for esterification of glycerol with acetic acid. Mineral acids such as H_2SO_4 , HCl , or H_3PO_4 were tried as homogeneous catalysts for esterification of glycerol [4–9]. However, the primary drawbacks associated with these homogeneous catalysts were catalyst separation, product purity, necessity of neutralization, and reactor corrosion [5]. Therefore, several studies focused on the development of various heterogeneous catalysts such as zeolites [3,10], heteropolyacids [5,7], SBA-15 [8], sulfated carbon nanotubes [11], zirconia [12], activated carbon [5], and sulfated metal oxides [11,13,14] for the esterification of glycerol with acetic acid. Recently, Amberlyst and ion exchange resins have been shown as effective catalysts in the presence of excess of glycerol [2–4,10,15–17].

Despite the significance of the reaction, minimal research attention has been devoted to the reaction kinetic study of glycerol acetylation reaction with acetic acid [4,18–20]. Reaction kinetic modeling and estimation of kinetic parameters are essential toward robust catalyst design, scale-up, and optimization of chemical process. Previous studies [4,20] reported acetylation of glycerol with acetic acid as a combination of series-parallel reaction pathways. Zhou et al. [4] studied the reaction kinetics of acetylation of glycerol with acetic acid by using Amberlyst-15 as catalysts. The first-order consecutive series reaction scheme was proposed, and the results obtained indicated that the apparent reaction rate constants for all the reactions were influenced by the initial mole ratio of acetic acid and glycerol. Khayoon et al. [18] proposed that the reaction followed consecutive series reaction pathway producing MAG, DAG, and TAG with surface reaction as the rate-limiting step. Patel and Singh [19] reported that the esterification reaction followed first-order kinetics, and the rates were not mass transfer limited in the presence of 1,2-tungstophosphoric acid anchored to different supports. Most of the previous works [4,18,20] reported the first-order rate equation for acetylation of glycerol. Mufrodi et al. [20] suggested that, in the presence of sulfuric acid, triacetyl glycerol synthesis was an exothermic reaction, and hence higher temperatures ($>118^\circ\text{C}$) were not beneficial. In addition, they have also found that the selectivity to triacetin decreased at high temperature ($>115^\circ\text{C}$) due to the evaporation of acetic acid. The most popular mechanistic model re-

ported in the literature is the Langmuir–Hinshelwood–Hougen–Watson (LHHW) model [4,18,19,21]. The LHHW model is identified as the most reliable model, which describe the catalytic reaction with high accuracy and produce the rate equations consistent with the kinetic data within the experimental error. However, in all the previous studies, the LHHW model is oversimplified by neglecting the resistance offered by the adsorption and desorption steps during the reaction and the simplified LHHW model reduced to the simple Power law model. Therefore, the development of the kinetic model by following the more realistic LHHW approach is important for fundamental understanding of the reaction kinetics of the glycerol acetylation reaction.

Mathematical modeling of chemical reaction kinetics and estimation of kinetic parameters often end up in the problem of nonlinear parameter estimation. Application of efficient optimization techniques is a key factor in obtaining physically significant kinetic parameters, which are estimated by minimizing the sum of squared deviation between experimental and simulated concentrations of reacting species. Improper choice of initial guess for model parameters results in nonoptimal solutions in turn giving unrealistic values for the model parameters. In this context, genetic algorithm (GA) provides a lot of robustness and the application of GA in problems of chemical kinetics is very promising [22–28]. The traditional algorithms that are based on the evaluation of derivatives fail in case of discontinuous functions or if derivatives do not exist. Other methods such as enumerative techniques—both random search and grid search methods become computationally expensive for problems involving a large number of variables in the objective function. Unlike most of the conventional optimization techniques, GA does not require the evaluation of derivatives nor does it need any other auxiliary information such as initial guess [22]. Therefore, GA is an ideal optimization technique for parameter estimation in cases where large uncertainty exists in model parameters and difficult to make an initial guess. GA evaluates the objective function at different points in a population simultaneously and selects the best solutions during each iteration. The population with best solutions evolves to reach the global optimum point.

In this study, a reaction pathway for the acetylation of glycerol with a sulfated alumina catalyst is proposed based on the experimental observations. The kinetic parameters were estimated based on the LHHW model with proper validation for assumptions. Nonlinear parameter estimation was performed using the GA optimization technique at the optimized reaction conditions presented in our previous work [29].

EXPERIMENTAL

Catalyst Synthesis

The details of catalyst synthesis and characterization are reported in our previous study [29,30]. The esterification reactions were carried out at atmospheric pressure in a round-bottom flask equipped with reflux and a magnetic stirrer. Acetic acid (99.5%; Rankem, India) and glycerol (99.9%; Merck Specialities, India) of required mole ratio was initially charged into the round-bottom flask. Both stirrer and heater were started immediately after the introduction of the feed. After reaching the desired temperature, a required amount of catalyst was added into the reactor and started to count the reaction time. The kinetic experiments were performed at the optimized reaction condition, i.e., in the presence of acetic acid to glycerol mole ratio of 12:1, 0.36 g of catalyst in the temperatures range of 80–110 °C [29]. Products samples were collected at a regular interval of 30 min for 5 h. Collected product samples were filtered, cooled, and then analyzed in a gas chromatograph (Newchrom GC, 6800, India) equipped with an AB-PONA (50 m × 0.2 mm) column and a flame ionization detector. The error in the GC measurements are assumed to be normally distributed with zero mean and 0.05 standard deviation (σ_{ci}). For quantification of products, the standard calibration curves were prepared using pure compounds (monoacetylglycerol (50%; Alfa Aesar, UK), diacetylglycerol (50%; Alfa Aesar, UK), and triacetylglycerol (99%; Alfa Aesar, UK)) and *n*-butanol (99%; Rankem, India) was used as the internal standard for the calculation of product moles. The conversion of glycerol and selectivity to different products were calculated based on the following definitions:

$$\text{Glycerol conversion (\%)} = \frac{\{(\text{Moles of glycerol converted}) / (\text{Initial moles of glycerol})\} \times 100}{(1)} \quad (1)$$

Selectivity of MAG, DAG or TAG (%) =

$$\frac{\{(\text{Moles of MAG, DAG or TAG formed}) / (\text{Total moles of MAG + DAG + TAG})\} \times 100}{(2)}$$

RESULTS AND DISCUSSION

Mass and Heat Transport Effects

To verify the external mass transfer limitation, the experiments were carried out at three different stirring speeds of 300, 500, and 700 rpm, respectively. The glycerol conversion and the products selectivity obtained are summarized in Table I. Results showed that the obtained glycerol conversion, products selectivity, and the calculated reaction rate at different stirring speed were almost unaffected (Table I). Therefore, for this kinetic study, the stirring speed was kept constant at 500 rpm with the assumption that resistance to external mass transfer is almost negligible at this stirring speed.

To verify the resistance offered by internal pore diffusion, a theoretical approach using the Weisz–Prater criterion has been used. This criterion uses measured values of the reaction rate to check if pore diffusion is limiting the overall rate. According to this criterion, internal mass transfer effects can be neglected when the value of certain parameter “ φ ” is less than 1, where φ is defined as follows. $\varphi = \frac{r_{obs} \rho_p R_p^2}{D_e C_s}$. In the present study, the calculated value of φ was found to be 2.944×10^{-11} at 80°C, which suggested the negligible effect of internal diffusion on the rate of reaction (Table II).

The acetylation of glycerol with acetic acid has been reported as an exothermic reaction [20]; however, in this study no significant variation of reaction temperature was observed during the course of experiments, which led to the assumption of isothermal reaction condition. To verify the thermal homogeneity in the reaction mixture, the experiments were performed at different stirring speeds. The results showed

Table I Variation of Glycerol Conversion and Products Selectivity at Different Stirring Speed

Stirring Speed (rpm)	Glycerol Conversion (%)	Selectivity (%)			Reaction Rate (molcat ⁻¹ h ⁻¹)
		MAG	DAG	TAG	
300	98.7	23.3	49.2	27.5	4.1×10^{-3}
500	99.2	22.8	49.8	27.4	4.3×10^{-3}
700	98.6	23.3	49.2	27.5	3.9×10^{-3}

Reaction condition: Acetic acid to glycerol mole ratio = 12:1, reaction temperature = 110°C, and catalyst amount = 0.36 g.

Table II Calculation of Weisz-Prater Criterion [31,32]

Symbol	Term	Value
R_p	Radius of catalyst particle	16.9×10^{-7} cm
ρ_p	True density of the catalyst	$2 \text{ g (cm}^3\text{)}^{-1}$
r_{obs}	Observed reaction rate at bulk concentration	1.6×10^{-7} mol glycerol gcat $^{-1}$ s $^{-1}$
C_s	Concentration of reactant (glycerol) at the external surface of the catalyst	1.02×10^{-3} mol (cm 3) $^{-1}$
T	Reaction temperature	353 K
M	Molecular weight of reactant (glycerol)	92.5 g mol $^{-1}$
a	Pore radius	19.2×10^{-8} cm
D_k	Knudsen diffusivity = $9.7 \times 10^3 \times a [T/M]^{1/2}$	362.9×10^{-5} cm 2 s $^{-1}$
ε	Porosity of catalyst	0.024
ζ	Tortuosity of catalyst = $1 - 0.5 \ln \varepsilon$	2.9
σ	Constriction factor	1.0
D_e	Effective diffusivity = $[D_k \varepsilon \sigma] / \zeta$	2.95×10^{-5} cm 2 s $^{-1}$
φ	Weisz-Prater criterion = $[r_{\text{obs}} \rho_p R_p^2] / D_e C_s$	2.94×10^{-11}

Table III Calculation of Prater Number

Symbol	Term	Value
$-\Delta H_{Rx}$	Heat of reaction	797.36 kJ mol $^{-1}$
λ_S	Thermal conductivity of catalyst pellet	0.2769 W m $^{-1}$ K $^{-1}$
λ_f	Average thermal conductivity of reacting mixture	0.1563 W m $^{-1}$ K $^{-1}$
λ_{eff}	Effective thermal conductivity of the catalyst pellet = $\lambda_S (\frac{\lambda_f}{\lambda_S})^\varepsilon$	0.2732 W m $^{-1}$ K $^{-1}$
C_s	Concentration of reactant (glycerol) at the external surface of the catalyst	1.019×10^{-3} mol (cm 3) $^{-1}$
T_S	Surface temperature	353 K
D_e	Effective diffusivity = $\frac{D_k \varepsilon \sigma}{\tau}$	2.951×10^{-5} cm 2 s $^{-1}$
ΔT	Maximum temperature difference = $T_{\text{max}} - T_S = \frac{-\Delta H_{Rx} D_e C_{AS}}{\lambda_{eff}}$	8.77

insignificant variation of glycerol conversion and products selectivity (Table I). Further, the Prater number was also calculated (Table III) [31–34]. The calculated temperature difference ($T_{\text{max}} - T_S$) within the catalyst particle was found to be low (~ 8.77 °C). This results also demonstrated the thermal homogeneity of the reaction mixture.

Catalytic Activity

The details of catalytic characterization and activity for esterification of glycerol over sulfated alumina catalysts having different compositions are reported in our previous study [29,30]. Among all the sulfated alumina catalyst examined, 2M $\text{SO}_4^{2-}/\gamma\text{-Al}_2\text{O}_3$ catalyst showed the highest catalytic activity and stability; hence this catalyst was chosen for a detailed kinetic study by varying the reaction times as well as reac-

tion temperature at the optimum acetic acid to glycerol mole ratio of 12:1 and in the presence of 0.36 g of catalyst. Over 2M $\text{SO}_4^{2-}/\gamma\text{-Al}_2\text{O}_3$ catalyst, the main reaction products were MAG, DAG, and TAG and the variation of concentration of glycerol, MAG, DAG, and TAG with reaction time and at different temperatures is shown in Fig. 1. In all the experiments, the concentration of glycerol was found to decrease with reaction time and almost complete conversion of glycerol was achieved within 3 h of reaction at 80°C. With increasing temperature, complete glycerol conversion was achieved within 30 min of reaction. The concentration of MAG and DAG passed through maxima, whereas the concentration of TAG increased with reaction time. However, with increasing temperature, the concentration of MAG and DAG passed through a maximum primarily after a runtime of 50 min whereas the concentration of TAG followed an increasing trend with reaction time as well as temperature. The

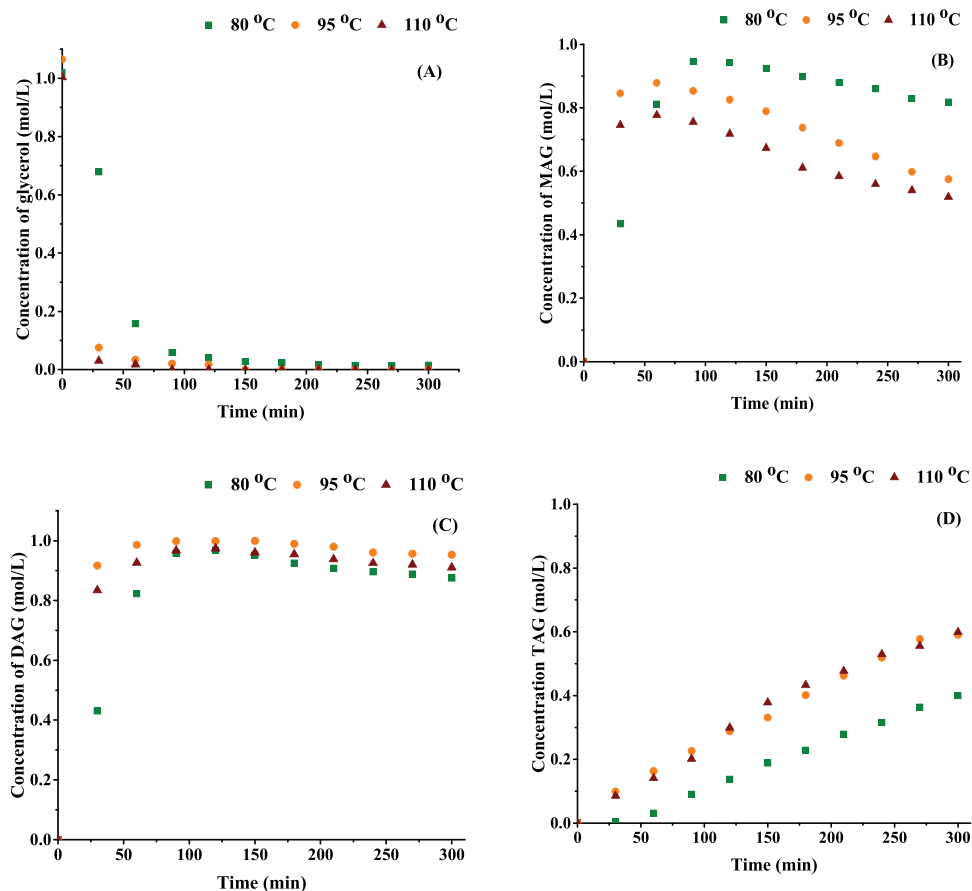


Figure 1 Variation of concentration (experimental) with time at different temperatures and at the acetic acid to glycerol mole ratio of 12:1 (A) glycerol, (B) MAG, (C) DAG, and (D) TAG. [Color figure can be viewed at wileyonlinelibrary.com]

concentration of TAG was almost similar at a temperature of 95 °C and higher. At all the temperatures, MAG was the dominating product at the initial stages of the reaction and with the course of reaction time, the concentration of MAG dropped whereas the concentrations of DAG and TAG increased. However, after reaching a maximum value, the concentration of DAG decreased slightly toward the end of the reaction. After 5 h of reaction time in all the experiments, DAG was the dominant product. It is also clear from Fig. 1 that both MAG and DAG reached the maximum concentration at the same time regardless of the reaction temperature, which suggested that the initial reaction might have followed a parallel route, i.e., glycerol might have directly converted to MAG and DAG followed by the conversion of MAG to DAG and DAG to TAG due to further acetylation. Therefore, based on the experimental observation, we propose a combination of a series–parallel pathway for glycerol acetylation (Fig. 2).

Development of the LHHW Mechanistic Kinetic Model

In this study, the LHHW model based on a dual site mechanism is used to describe the kinetics of acetylation of glycerol over a sulfated alumina catalyst. External and internal diffusion of mass and heat transfer effect was neglected based on the value obtained for the Weisz–Prater criterion (Table II) and Prater number (Table III). Therefore, the LHHW model was developed based on the adsorption, desorption, and surface reaction steps only. To develop the kinetic model, it is assumed that, initially, both the reactants—glycerol and acetic acid—diffused from the bulk liquid phase to the external surface of the catalyst and gets adsorbed. In the second step, the adsorbed molecules at the catalyst surface react with each other to form the products at the catalyst surface. Finally, the products are desorbed from the surface followed by the diffusion to the bulk liquid phase. Thus for model development, in addition to the surface reactions step, the impact of resistance

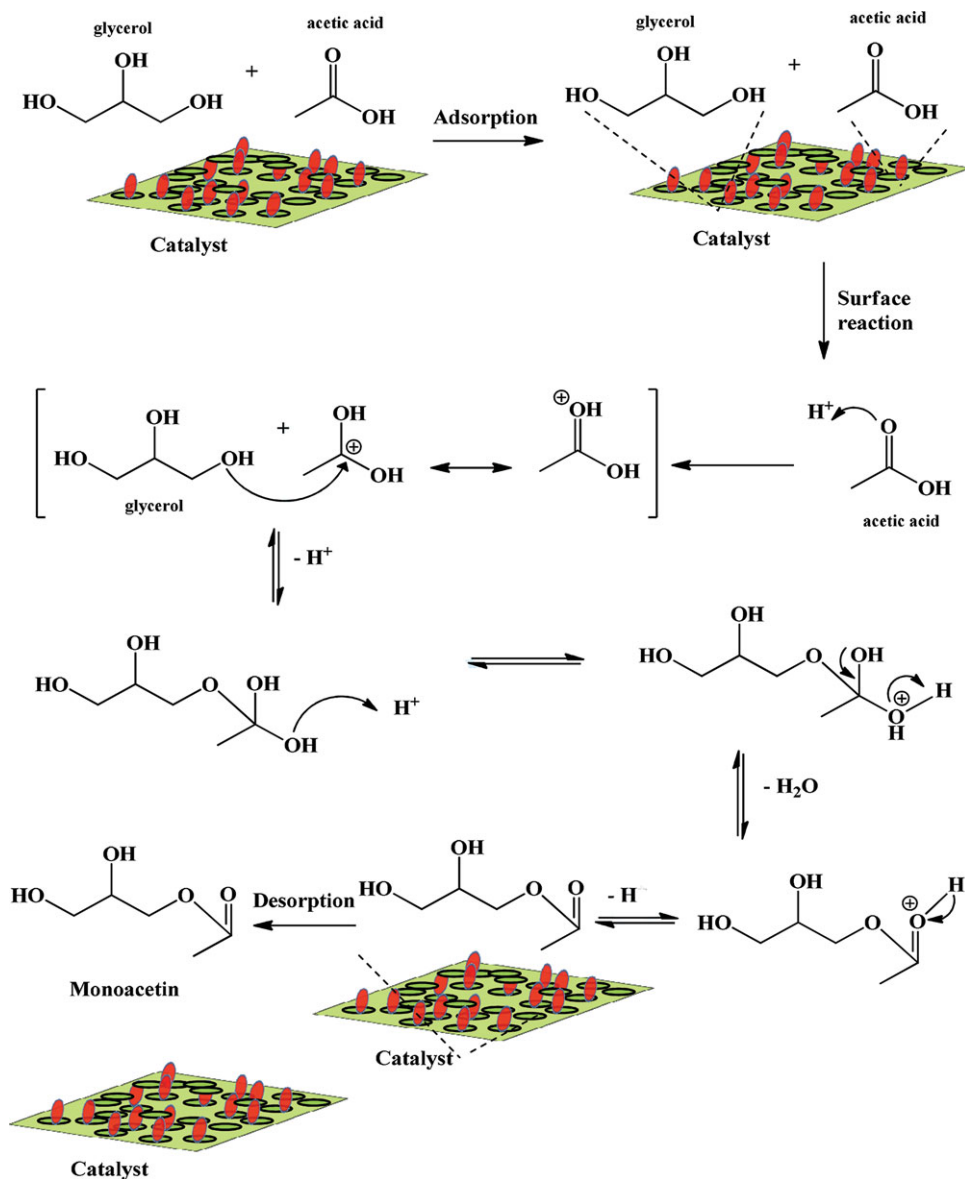


Figure 3 Reaction mechanism of glycerol acetylation with acetic acid to MAG over $2\text{MSO}_4^{2-}/\gamma\text{-Al}_2\text{O}_3$ catalyst. [Color figure can be viewed at wileyonlinelibrary.com]

pathway. This was accomplished by the nucleophilic attack of the hydroxyl group of MAG and DAG on the positively charged carbon atom of acetic acid. However, it was inferred that the formation of DAG was also possible from the direct acetylation of glycerol in which two hydroxyl groups of glycerol simultaneously reacted with two molecules of acetic acid containing the positively charged carbon atom followed by the removal of two molecules of water and subsequent deprotonation to form DAG. The mechanism clearly showed that the proton from the solid cata-

lyst initiated the reaction, and this signifies the role of acidity in this reaction. The mechanism also suggested that the proton from the catalyst get restored toward the end of each reaction, facilitating the adequate number of acidic sites on the catalyst always available with a specific amount of catalyst. Hence an excess amount of catalyst cannot improve catalyst activity.

The reaction mechanism for acetylation of glycerol with acetic acid to produce MAG, DAG, and TAG can be represented by the following steps:

Step 1: Adsorption of acetic acid (A) on the vacant site (S) of catalyst:



Adsorption of glycerol (G) on the vacant site (S) of catalyst:



Step 2: The surface reaction between adsorbed glycerol (GS) and acetic acid (AS) to produce adsorbed MAG (MS) and DAG (DS) on the surface of the catalyst. Further, adsorbed MAG and DAG reacted with adsorbed acetic acid to produce adsorbed DAG and TAG, respectively.



Step 3: Desorption of MAG (M), DAG (D), and TAG (T) from the catalyst surface created a vacant site as follows:



The following assumptions were made to derive the simplified rate expression:

1. The resistance offered by mass transfer (internal and external) and internal heat transfer was found to be negligible, and hence the surface reaction is assumed to be the rate-controlling step under isothermal conditions.

2. In all the experiments, acetic acid was in large excess (acetic acid/glycerol mole ratio = 12:1), the conversion of acetic acid was only 10–15% after 5 h. Hence, it is assumed that the concentration of acetic acid C_A remains constant and the pseudo–first-order reaction is assumed.
3. No catalyst deactivation was observed [29], and hence the concentration of coproduced water is neglected and the activity of catalyst is assumed to be constant.
4. Adsorption and desorption steps were assumed to be fast and in equilibrium.
5. The acetylation reaction is assumed to be irreversible.

The final rate expressions were developed through the following steps:

$$(-r_1) = k_1 \left(C_G C_S - \frac{C_{GS}}{K_1} \right); \quad K_1 = \frac{k_1}{k_{-1}} \quad (11)$$

$$(-r_2) = k_2 \left(C_A C_S - \frac{C_{AS}}{K_2} \right); \quad K_2 = \frac{k_2}{k_{-2}} \quad (12)$$

$$(-r_3) = k_3 \left(C_{GS} C_{AS} - \frac{C_{MS} C_{DS} C_S}{K_3} \right); \quad K_3 = \frac{k_3}{k_{-3}} \quad (13)$$

$$(-r_4) = k_4 \left(C_{MS} C_{AS} - \frac{C_{DS} C_S}{K_4} \right); \quad K_4 = \frac{k_4}{k_{-4}} \quad (14)$$

$$(-r_5) = k_5 \left(C_{DS} C_{AS} - \frac{C_{TS} C_S}{K_5} \right); \quad K_5 = \frac{k_5}{k_{-5}} \quad (15)$$

$$(-r_6) = k_6 \left(C_{MS} - \frac{C_M C_S}{K_6} \right); \quad K_6 = \frac{k_6}{k_{-6}} \quad (16)$$

$$(-r_7) = k_7 \left(C_{DS} - \frac{C_D C_S}{K_7} \right); \quad K_7 = \frac{k_7}{k_{-7}} \quad (17)$$

$$(-r_8) = k_8 \left(C_{TS} - \frac{C_T C_S}{K_8} \right); \quad K_8 = \frac{k_8}{k_{-8}} \quad (18)$$

$$C_{\text{Total}} = C_S + K_1 C_G C_S + K_2 C_A C_S + \frac{C_M C_S}{K_6} + \frac{C_D C_S}{K_7} + \frac{C_T C_S}{K_8} \quad (19)$$

$$C_S = \frac{C_{\text{Total}}}{\left(1 + K_1 C_G + K_2 C_A + \frac{C_M}{K_6} + \frac{C_D}{K_7} + \frac{C_T}{K_8}\right)} \quad (20)$$

$$(-r_3) = k_3 C_{GS} C_{AS} = \frac{k_3 K_1 K_2 C_G C_A C_{\text{Total}}^2}{\left(1 + K_1 C_G + K_2 C_A + \frac{C_M}{K_6} + \frac{C_D}{K_7} + \frac{C_T}{K_8}\right)^2} \quad (21)$$

$$(-r_4) = k_4 C_{MS} C_{AS} = \frac{\frac{k_4 K_2}{K_6} C_M C_A C_{\text{Total}}^2}{\left(1 + K_1 C_G + K_2 C_A + \frac{C_M}{K_6} + \frac{C_D}{K_7} + \frac{C_T}{K_8}\right)^2} \quad (22)$$

$$(-r_5) = k_5 C_{DS} C_{AS} = \frac{\frac{k_5 K_2}{K_7} C_D C_A C_{\text{Total}}^2}{\left(1 + K_1 C_G + K_2 C_A + \frac{C_M}{K_6} + \frac{C_D}{K_7} + \frac{C_T}{K_8}\right)^2} \quad (23)$$

$$(-r_3) = k_3 C_{GS} C_{AS} = \frac{k_3 K_1 K_2 C_G C_A C_{\text{Total}}^2}{\left(1 + K_1 C_G + K_2 C_A + \frac{C_M}{K_6} + \frac{C_D}{K_7} + \frac{C_T}{K_8}\right)^2} = \frac{k'_3 C_G}{\left(1 + K_1 C_G + K_2 C_A + \frac{C_M}{K_6} + \frac{C_D}{K_7} + \frac{C_T}{K_8}\right)^2} \quad (24)$$

$$(-r_4) = k_4 C_{MS} C_{AS} = \frac{\frac{k_4 K_2}{K_6} C_M C_A C_{\text{Total}}^2}{\left(1 + K_1 C_G + K_2 C_A + \frac{C_M}{K_6} + \frac{C_D}{K_7} + \frac{C_T}{K_8}\right)^2} = \frac{k'_4 C_M}{\left(1 + K_1 C_G + K_2 C_A + \frac{C_M}{K_6} + \frac{C_D}{K_7} + \frac{C_T}{K_8}\right)^2} \quad (25)$$

$$(-r_5) = k_5 C_{DS} C_{AS} = \frac{\frac{k_5 K_2}{K_7} C_D C_A C_{\text{Total}}^2}{\left(1 + K_1 C_G + K_2 C_A + \frac{C_M}{K_6} + \frac{C_D}{K_7} + \frac{C_T}{K_8}\right)^2} = \frac{k'_5 C_D}{\left(1 + K_1 C_G + K_2 C_A + \frac{C_M}{K_6} + \frac{C_D}{K_7} + \frac{C_T}{K_8}\right)^2} \quad (26)$$

where k'_3 , k'_4 , and k'_5 are apparent reaction rate constants.

Estimation of Kinetic Parameters

The mathematical model for the batch reactor was developed using the unsteady state material balance for each component as follows:

$$\begin{aligned} \text{Net rate of disappearance of glycerol, } (-r_G) \\ = \frac{-dC_G}{dt} = (-r_3) \frac{m_C}{V} \end{aligned} \quad (27)$$

$$\begin{aligned} \text{Net rate of formation of MAG, } (r_M) \\ = \frac{dC_M}{dt} = [(-r_3) - (-r_4)] \frac{m_C}{V} \end{aligned} \quad (28)$$

$$\begin{aligned} \text{Net rate of formation of DAG, } (r_D) \\ = \frac{dC_D}{dt} = [(-r_3) + (-r_4) - (-r_5)] \frac{m_C}{V} \end{aligned} \quad (29)$$

$$\begin{aligned} \text{Net rate of formation of TAG, } (r_T) \\ = \frac{dC_T}{dt} = (-r_5) \frac{m_C}{V} \end{aligned} \quad (30)$$

where m_C is the weight of the catalyst and V is the total reactant volume.

For the optimization, the objective function f was defined as follows:

$$f = \sum_{i=1}^N \left[\left(C_{G,\text{exp}}^i - C_{G,\text{sim}}^i \right)^2 + \left(C_{M,\text{exp}}^i - C_{M,\text{sim}}^i \right)^2 + \left(C_{D,\text{exp}}^i - C_{D,\text{sim}}^i \right)^2 + \left(C_{T,\text{exp}}^i - C_{T,\text{sim}}^i \right)^2 \right] \quad (31)$$

where N is the number of samples and C_{exp}^i and C_{sim}^i are the experimental and simulated concentrations for glycerol, MAG, DAG, and TAG, respectively.

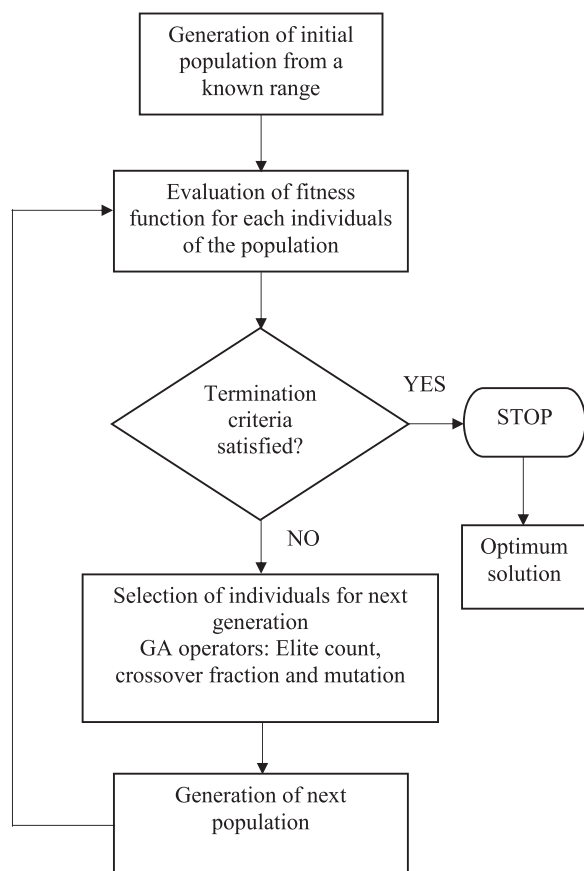


Figure 4 A simplified schematic flow diagram describing GA.

The kinetic model represented by the set of ordinary differential equations (ODE; Eqs. (27)–(30)) were first solved using the Rosenbrock algorithm (ode23s) in MATLAB. This ODE solver function was nested to the main GA optimization function. The GA optimization was triggered by the generation of initial population of size 1000 for the rate constants. The parameters were searched within positive real numbers. The resultant values for the concentrations of reacting species at specified time intervals were used in the least-square objective function (Eq. (31)). The best points with least values of the objective function were selected using the selection function. Along with the selection function with an elite count of (0.05*population size), an optimum crossover fraction of 0.8 was used to generate the next population. The termination criteria for the algorithm was chosen based on the fitness limit and function tolerance. The algorithm stopped when either of the two conditions satisfied: The value of the fitness function for the best point in a population becomes less than or equal to fitness limit or when the average change in the value of fitness function for a specific number of generations becomes less than the

function tolerance. The values of the fitness limit and the function tolerance were fixed at 1×10^{-3} and 1×10^{-5} , respectively. The simplified GA optimization algorithm is described in Fig. 4.

The simulated concentrations at different reaction temperature were compared with the experimentally observed concentrations (Fig. 5). Results suggested that the model is very much consistent with the kinetic data, producing good fit between the experimental and estimated concentrations of all species. The descriptive capability of the model with the estimated parameters was verified using the coefficient of determination (R^2) and by the lack-of-fit (LOF) test. The coefficient of determination (R^2) compared the overall fit of the model with that of representing the model as the average of all experimental observations. The LOF test compared the calculated weighted residuals (χ^2) value with the reference χ^2 with ($N \times M - P$) degrees of freedom and 95% confidence interval (where N is the number of sample points, M is the number of measured responses, and P is the number of estimated model parameters) [35]. The definition of R^2 and χ^2 is provided in Eqs. (32) and (33), respectively. As shown in Table IV, the value of R^2 is close to unity and the weighted residuals less than the reference χ^2 indicated adequate representation of data by the model.

$$R_i^2 = 1 - \frac{\sum_{j=1}^N (C_{ij,\text{exp}} - C_{ij,\text{pred}})^2}{\sum_{j=1}^N (C_{ij,\text{exp}} - \bar{C}_i)^2}; \quad i = 1 \text{ to } M \quad (32)$$

$$\chi^2 = \sum_{i=1}^M \sum_{j=1}^N \frac{(C_{ij,\text{exp}} - C_{ij,\text{pred}})^2}{\sigma_{C_{i,\text{exp}}}^2} \quad (33)$$

The estimated values of rate constants, k'_3 , k'_4 and k'_5 , are shown in Table V. The values of rate constants followed the order $k'_3 > k'_5 > k'_4$ at all three temperatures. In fact, the value of k'_3 was much larger with respect to k'_4 and k'_5 whereas the values of k'_4 and k'_5 were almost close. This agrees with the experimental observations: DAG as the dominant product is followed by TAG and MAG after 5 h of reaction time. Similar results were reported earlier for acetylation of glycerol in the presence of Amberlyst catalyst at the acetic acid to glycerol mole ratio of 3:1 [4]. In addition, the increase in reaction temperature improved the values of rate constants and enabled the concentrations of both glycerol and DAG to reach the equilibrium much faster almost within 100 min of reaction time (Fig. 1). The estimated rate constants were used to obtain the activation energy and preexponential factor using the Arrhenius equation (Fig. 6), and the obtained

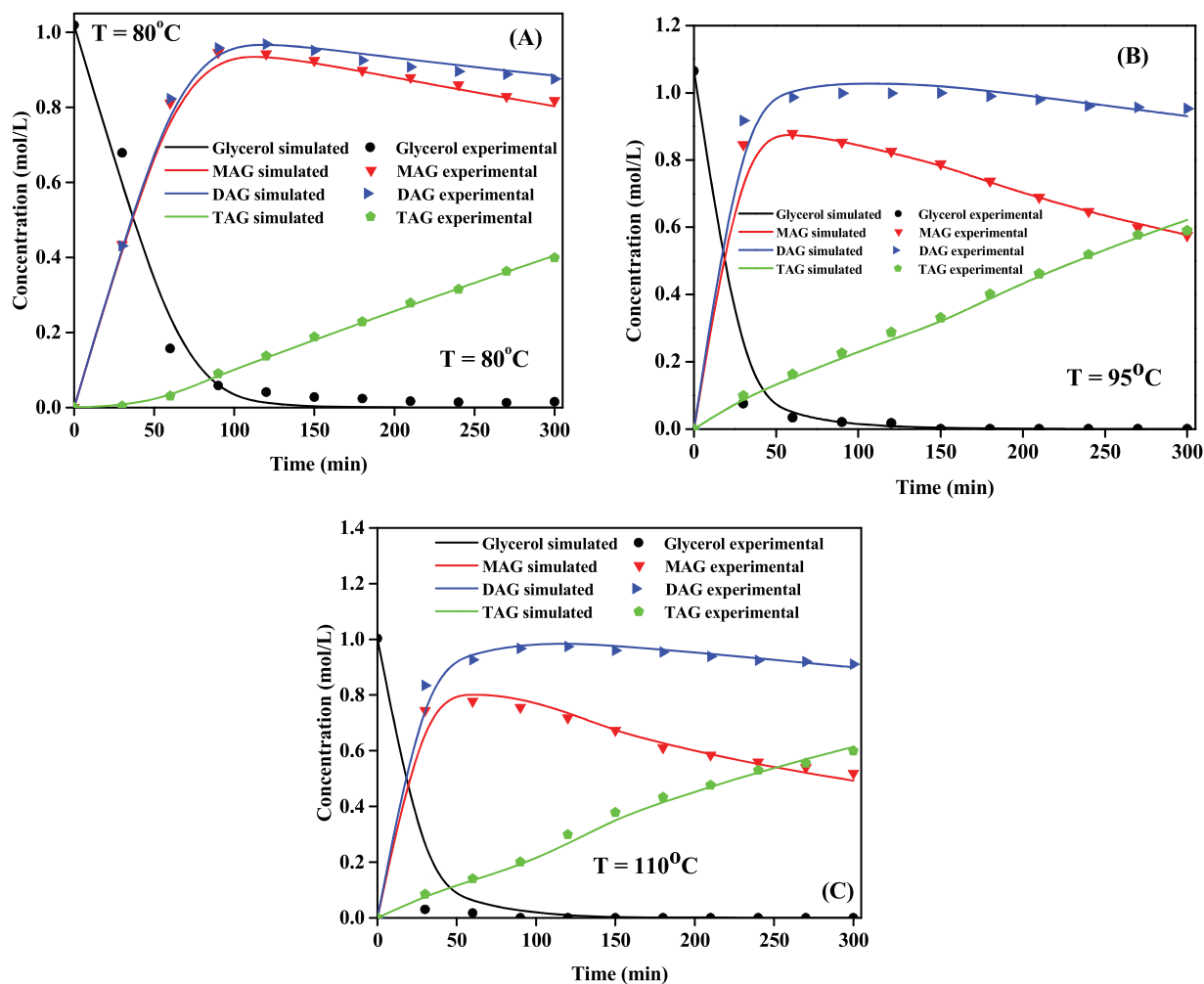


Figure 5 Comparison of experimentally observed concentration and simulated concentration at the acetic acid to a glycerol mole ratio of 12:1 and at different reaction temperature (A) at 80°C, (B) at 95°C, and (C) at 110°C. [Color figure can be viewed at wileyonlinelibrary.com]

Table IV Statistical Analysis of Parameter Estimation in Terms of LOF Test and R^2

Temperature (°C)	R^2				Weighted Residuals	Ref. χ^2 (95%)
	Glycerol	MAG	DAG	TAG		
80	0.988	0.998	0.998	0.999	6.331	50.998
95	0.998	0.999	0.995	0.994	3.675	50.998
110	0.986	0.988	0.996	0.993	9.827	50.998

results are shown in Table VI. The activation energies for direct acetylation of glycerol to MAG and DAG, acetylation of MAG to DAG, and acetylation of DAG to TAG were found to be 7.2, 37.1, and 26.6 kJ mol⁻¹, respectively. The activation energy values were consistent with the results reported earlier for the acetylation of glycerol to MAG, MAG to DAG, and DAG to

Table V Values of Apparent Reaction Rate Constants at Different Temperatures

Temperature (°C)	k'_3 (h ⁻¹)	k'_4 (h ⁻¹)	k'_5 (h ⁻¹)
80	1.3658	0.0401	0.0616
95	1.4871	0.0589	0.0985
110	1.6555	0.1082	0.1249

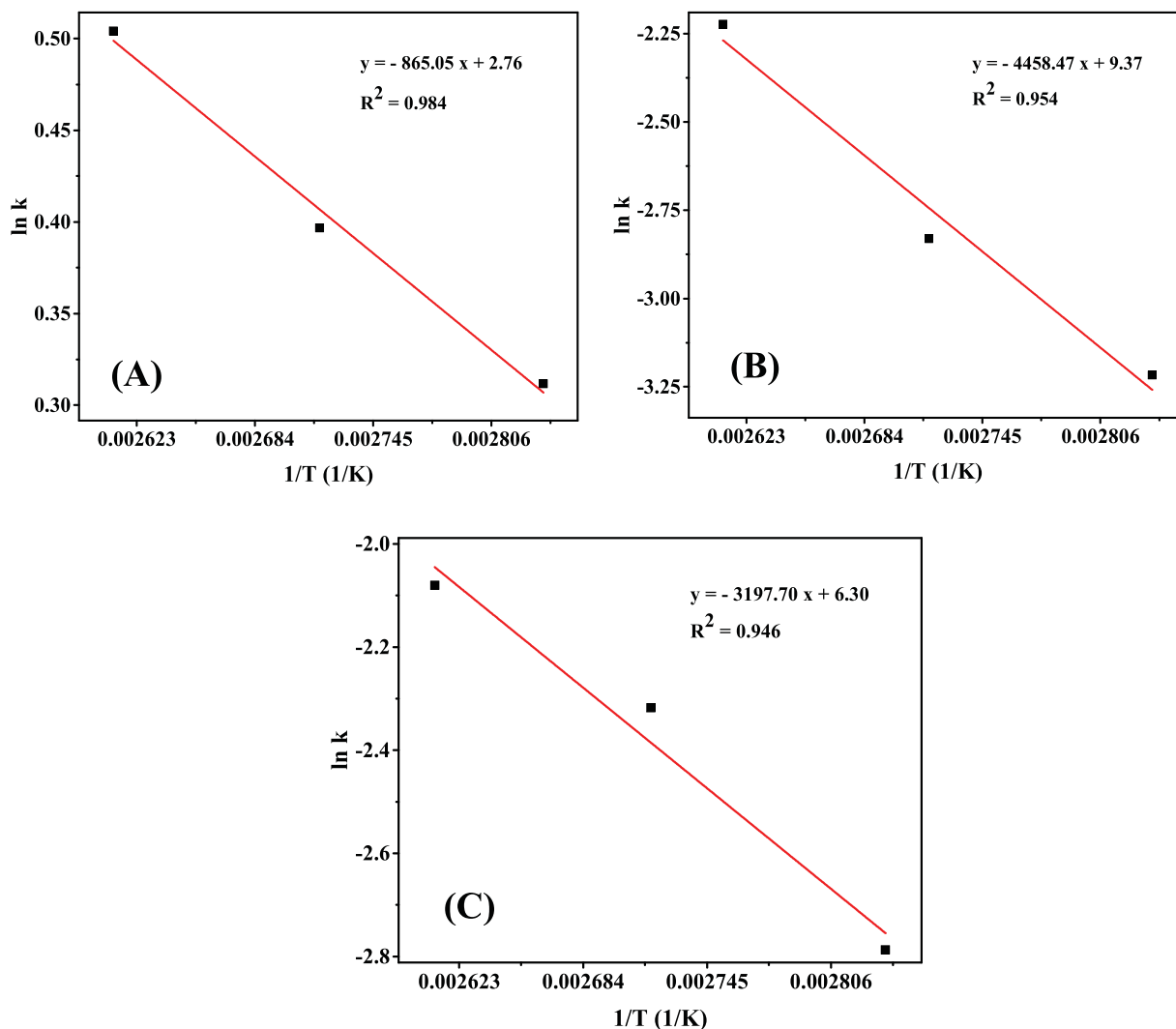


Figure 6 Arrhenius plot to calculate activation energy for (A) acetylation of glycerol to MAG and DAG, (B) acetylation of MAG to DAG, and (C) acetylation of DAG to TAG. [Color figure can be viewed at wileyonlinelibrary.com]

Table VI Estimated Values of Kinetic Parameters

Kinetic Parameters	For Glycerol		
	to MAG and DAG	For MAG to DAG	For DAG to TAG
Activation energy, E_a (kJ mol ⁻¹)	7.2	37.1	26.6
Pre-exponential factor, k_0 (h ⁻¹)	15.8	11731.1	544.6

TAG by using sulfuric acid as a catalyst [20]. The high values of activation energy and pre-exponential factor for the acetylation of MAG to DAG and DAG to TAG suggested that higher temperature facilitated the product distribution toward higher esters [4]. The high value

of reaction rate constant and low value of activation energy for the direct acetylation of glycerol to MAG and DAG explained the rapid rate of formation of these products at the initial stages of the reaction (Tables V and VI).

CONCLUSIONS

A kinetic study of acetylation of glycerol was carried out with a highly active and stable 2M SO₄²⁻/γ-Al₂O₃ catalyst prepared by the impregnation method. The experimental study confirmed the reaction pathway as a combination of pseudo-first-order series and parallel reactions consisting of direct acetylation of glycerol to MAG and DAG followed by the conversion

of MAG to DAG and DAG to TAG, following series consecutive reaction pathway. The LHHW kinetic model was developed by considering the surface reaction as the rate-limiting step. Results showed that the model correlated the rate equations satisfactorily and produced good fit between the experimental and estimated concentrations of glycerol and products. The apparent reaction rate constants were determined by numerically solving the differential rate equations by using ode23 tool in MATLAB coupled with GA, which enabled the minimization of residual sum of squares between the experimentally observed concentrations and estimated concentrations for glycerol and products. The Arrhenius equation was used to calculate the activation energy and pre-exponential factor for the reactions from the estimated rate constants. The activation energy for direct acetylation of glycerol to MAG and DAG, acetylation of MAG to DAG, and acetylation of DAG to TAG was found to be 7.2, 37.1, and 26.6 kJ mol⁻¹, respectively. The activation energy was higher for the acetylation of MAG to DAG. However, DAG was also formed by the direct acetylation of glycerol, having low activation energy. As a result, DAG appeared as the dominant product.

NOMENCLATURE

C_A	Concentration of acetic acid at any time, mol L ⁻¹	k_{-3}	Backward reaction rate constant for acetylation of glycerol to MAG and DAG, h ⁻¹
C_{AS}	Concentration of acetic acid at catalyst surface	k_4	Forward reaction rate constant for acetylation of MAG to DAG, h ⁻¹
C_D	Concentration of DAG, mol L ⁻¹	k_{-4}	Backward reaction rate constant for acetylation of MAG to DAG, h ⁻¹
C_{DS}	Concentration of DAG at catalyst surface	k_5	Forward reaction rate constant for acetylation of DAG to TAG, h ⁻¹
C_G	Concentration of glycerol at any time, mol L ⁻¹	k_{-5}	Backward reaction rate constant for acetylation of DAG to TAG, h ⁻¹
$C_{G,S}$	Concentration of glycerol at catalyst surface	k_6	Forward reaction rate constant for desorption of MAG from catalyst active site, h ⁻¹
C_M	Concentration of MAG, mol L ⁻¹	k_{-6}	Backward reaction rate constant for desorption of MAG from the catalyst active site, h ⁻¹
C_{MS}	Concentration of MAG at catalyst surface	k_7	Forward reaction rate constant for desorption of DAG from catalyst active site, h ⁻¹
C_S	Concentration of the vacant sites	k_{-7}	Backward reaction rate constant for desorption of DAG from the catalyst active site, h ⁻¹
C_T	Concentration of TAG, mol L ⁻¹	k_8	Forward reaction rate constant for desorption of DAG from catalyst active site, h ⁻¹
C_{Total}	Total concentration of catalyst active sites	k_{-8}	Backward reaction rate constant for desorption of DAG from the catalyst active site, h ⁻¹
C_{TS}	Concentration of TAG at catalyst surface	K_1	Equilibrium constant for adsorption of glycerol on catalyst active site
E_a	Activation energy, kJ mol ⁻¹	K_2	Equilibrium constant for adsorption of acetic acid on catalyst active site
k_0	Pre-exponential factor, h ⁻¹	K_3	Equilibrium constant for acetylation of glycerol to MAG
k_1	Forward reaction rate constant for adsorption of glycerol on catalyst active site, h ⁻¹	K_4	Equilibrium constant for acetylation of MAG to DAG
k_{-1}	Backward reaction rate constant for the adsorption of glycerol on the catalyst active site, h ⁻¹	K_5	Equilibrium constant for acetylation of DAG to TAG
k_2	Forward reaction rate constant for adsorption of acetic acid on catalyst active site, h ⁻¹	K_6	Equilibrium constant for desorption of MAG from catalyst active site
k_{-2}	Backward reaction rate constant for the adsorption of acetic acid on the catalyst active site, h ⁻¹	K_7	Equilibrium constant for desorption of DAG from catalyst active site
k_3	Forward reaction rate constant for acetylation of glycerol to MAG and DAG, h ⁻¹	K_8	Equilibrium constant for desorption of TAG from catalyst active site
		k'_3	Apparent reaction rate constant for acetylation of glycerol to MAG and DAG, h ⁻¹
		k'_4	Apparent reaction rate constant for acetylation of MAG to DAG, h ⁻¹
		k'_5	Apparent reaction rate constant for acetylation of DAG to TAG, h ⁻¹
		m_c	Weight of the catalyst, g
		R^2	Determination coefficient
		T	Reaction temperature, °C
		V	Total volume of reactants, L

Authors are thankful to Ministry of Human Resource Development (MHRD), Government of India for the award of fellowship to carry out this work in the Department of Chemical Engineering at Indian Institute of Technology Roorkee, Roorkee, India.

BIBLIOGRAPHY

- Acevedo, J. C.; Hernandez, J. A.; Valdes, C. F.; Khanal, S. K. *Bioresour. Technol.* 2015, 188, 117–123.
- Yang, F.; Hanna, M. A.; Sun, R. *Biotechnol. Biofuels* 2012, 5–13.
- Zhou, L.; Al-Zaini, E.; Adesina, A. A. *Fuel* 2013, 103, 617–625.
- Zhou, L.; Nguyen, T. H.; Adesina, A. A. *Fuel Process. Technol.* 2012, 104, 310–318.
- Ferreira, P.; Fonseca, I. M.; Ramos, A. M.; Vital, J.; Castanheiro, J. E. *Catal. Commun.* 2011, 12, 573–576.
- Sanchez, J. A.; Hernandez, D. L.; Moreno, J. A.; Mondragon, F.; Fernandez, J. J. *Appl. Catal. A: Gen.* 2011, 405, 55–60.
- Ferreira, P.; Fonseca, I. M.; Ramos, A. M.; Vital, J.; Castanheiro, J. E. *Appl. Catal. B: Environ.* 2009, 91, 416–422.
- Trejda, M.; Stawicka, K.; Dubinska, A.; Ziolek, M. *Catal. Today* 2012, 187, 129–134.
- Troncea, S. B.; Wuttke, S.; Kemnitz, E.; Coman, S. M.; Parvulescu, V. I. *Appl. Catal. B Environ.* 2011, 107, 260–267.
- Goncalves, V. L. C.; Pinto, B. P.; Silva, J. C.; Mota, C. J. A. *Catal. Today* 2008, 133, 673–677.
- Ji, X.; Chen, Y.; Wang, X.; Liu, W. *Kinet. Catal.* 2011, 52, 555–558.
- Dosuna-Rodriguez, I.; Adriany, C.; Gaigneaux, E. M. *Catal. Today* 2011, 167, 56–63.
- Mekhemer, G. A. H.; Khalaf, H. A.; Mansour, S. A. A.; Nohman, A. K. H. *Monatsh Chem/Chem Monthly* 2005, 136, 2007–2016.
- Yang, T.; Chang, T.; Yeh, C. J. *Mol. Catal. A: Chem.* 1997, 115, 339–346.
- Liao, X.; Zhu, Y.; Wang, S. G.; Li, Y. *Fuel Process. Technol.* 2009, 90, 988–993.
- Jagadeeswaraiyah, K.; Balaraju, M.; Prasad, P. S. S.; Lingaiah, N. *Appl. Catal. A: Gen.* 2010, 386, 166–170.
- Dosuna-Rodriguez, I.; Gaigneaux, E. M. *Catal. Today* 2012, 195, 14–21.
- Khayoon, M. S.; Triwahyono, S.; Hameed, B. H.; Jalil, A. A. *Chem. Eng. J.* 2014, 243, 473–484.
- Patel, A.; Singh, S. *Fuel* 2014, 118, 358–364.
- Mufrodi, Z.; Sutijan; Rochmadi; Budiman, A. *Int. J. Chem.* 2012, 4, 101–107.
- Okoye, P. U.; Abdullah, A. Z.; Hameed, B. H. *Renew Sustainable Energy Rev.* 2017, 74, 387–401.
- Bhaskar, V.; Gupta, S. K.; Ray, A. K. *Rev. Chem. Eng.* 2000, 16, 1–54.
- Mohan, S.; Singh, Y.; Verma, D. K.; Hasan, S. H. *Process Saf. Environ. Prot.* 2015, 96, 156–166.
- Abbasi, R.; Wu, L.; Wanke, S. E.; Hayes, R. E. *Chem. Eng. Res. Des.* 2012, 90, 1930–1942.
- Costa, C. B. B.; Rivera, E. A. C.; Alves, M. C.; Maciel, M. R. W.; Filho, R. M. *Chem. Eng. Sci.* 2007, 62, 4780–4801.
- Tsuchiya, M.; Ross, J. J. *Phys. Chem. A* 2001, 105, 4052–4058.
- Hernandez, J. J.; Ballesteros, R.; Sanz-Argent, J. *Math. Comput. Model.* 2010, 52, 1185–1193.
- Polifke, W.; Geng, W. Q.; Dobbeling, K. *Combust. Flame* 1998, 113, 119–134.
- Rane S. A., Pudi, S. M.; Biswas, P. *Chem. Biochem. Eng. Q.* 2016, 30, 33–45.
- Arun, P.; Pudi, S. M.; Biswas, P. *Energy Fuels* 2016, 30, 584–593.
- Fogler, H. S. *Elements of Chemical Reaction Engineering*, 4th ed., Chapter 4; Prentice Hall: Upper Saddle River, NJ, 2006.
- Thirumal bai, P.; Manokaran, V.; Saiprasad, P. S.; Srinath, S. *Proc. Eng.* 2015, 127, 1338–1345
- Mischke, R. A.; Smith, J. M. *Ind. Eng. Chem. Fundam.* 1962, 1, 288–292.
- Kolitcheff, S.; Jolimaitre, E.; Hugon, A.; Verstraete, J.; Carrette, P. L.; Fayolle, M. T. *Microporous Mesoporous Mater.* 2017, 248, 91–98.
- Bard, Y.; *Nonlinear Parameter Estimation*; Academic Press: New York, 1974.